

Comment on *Nature* 586, 373 (2020) by E. Snider *et al.*. Revised 19-2-2022

D. van der Marel^a and J. E. Hirsch^b

^a*Department of Quantum Matter Physics, University of Geneva,
24 Quai Ernest-Ansermet, 1211 Geneva, Switzerland and*

^b*Department of Physics, University of California, San Diego, La Jolla, CA 92093-0319, USA*

In Ref. [1] Snider *et al.* reported room temperature superconductivity in carbonaceous sulfur hydride (CSH) under high pressure. Recently the data for the temperature dependent ac magnetic susceptibility shown in figures of Ref. [1] have appeared in the form of tables corresponding to different pressures [2]. Here we analyze the data for a pressure of 160 GPa.

I. INTRODUCTION

In Ref. [1] it is reported that a material termed carbonaceous sulfur hydride (hereafter called CSH) is a room temperature superconductor. Data for resistance versus temperature and ac susceptibility versus temperature at six different pressures show drops suggesting superconducting transitions. Recently two of the authors of Ref. [1] have posted the numerical values of the data for the ac susceptibility curves presented in Ref. [1], as well as the underlying raw data, on arXiv [2]. The raw data and the data presented in Ref. [1] are called “Measured Voltage” and “Superconducting Signal” respectively in Ref. [2]. Here we give an analysis of the ac susceptibility data for pressure $p = 160$ GPa. Other analysis of the susceptibility data in Ref. [2] were presented in Refs. [3–5].

II. ANALYSIS OF THE 160 GPa DATA

Fig. 1a shows the susceptibility corresponding to pressure 160 GPa shown in Extended Data Figure 7d of Ref. [1]. The numerical values are given in the second column of Table 5 of Ref. [2] (labeled “Superconducting Signal”). A superconducting transition appears to take place around $T = 170$ K. In Fig. 1 panels c and d these data are shown on a 15 times expanded y -axis. Because of the steep rise at 170 K the regions above and below 170 K need to be displayed in separate panels. A similar zoom of the 160 GPa curve was previously shown in Fig. 9 of Ref. [5]. One of the striking features is a series of discontinuous steps. These steps are directly visible to the eye in the temperature ranges where $\chi'(T)$ has a weak temperature dependence. However, they are also present in the range where $\chi'(T)$ rises steeply as a function of temperature, as can be seen by calculating the difference between neighboring points

$$\Delta\chi(j) = \chi(T_j) - \chi(T_{j-1}). \quad (1)$$

This quantity, shown in Fig. 1 b, exhibits an intriguing “aliasing” effect in the “shadow curves” displaced vertically by integer multiples of 0.1655 (in section V this will be refined to 0.16555 ± 0.00005 by examining the noise

of the 3d and 4th derivatives). To make this crisp, the vertical axis of Fig. 1 b corresponds to $\Delta\chi(j)/0.16555$. Clearly this is a set of curves vertically offset by an integer $n = -1, 0, 1, 2, 3$ and 4. The most systematic offsets in sign and size occur between 169.6 K and 170.1 K.

By shifting continuous segments of the curves by an amount $0.16555n$, with n integers that can be read off from Fig. 1b, it is a simple and straightforward task to “unwrap” the vertical offsets [6]. The result for the two separate ranges above and below 170 K is displayed in Fig. 1 e and f, and for the full range in panel g. Comparing panel e to c, and f to d it is possible to verify that the resulting curves are extremely smooth and completely free of discontinuities. Comparing panel g to a the steep rise at 170 K is absent from panel g. As a consistency check $\Delta\chi(j)$ of panel g was finally calculated and is shown in panel h. Comparing the result shown in panel h with that in panel b (shown with the same vertical scale to facilitate comparison) it can be seen that there are no shadow curves in panel h, demonstrating that not only the temperature dependence of panel g is smooth, the differential shown in panel h is, surprisingly for an experimental quantity, also completely smooth.

The behavior of the data shown in Fig. 1 c and d, together with the fact that the segments can be joined by vertical shifts that are all of the same form $0.16555n$, indicates that the disconnected segments are portions of a continuous curve that has been broken up by quantized steps. The sequence of steps form together a quantized component which is entirely responsible for the steep rise of $\chi'(T)$ at 170 K seen in Fig. 1 a. The data (Superconducting Signal) of Fig. 1 a can be expressed as:

$$\begin{aligned} \text{Superconducting Signal} &= \text{quantized component} \\ &+ \text{unwrapped curve} \end{aligned} \quad (2)$$

where the unwrapped curve is given in Fig. 1 g. Fig. 2 shows the same information as panels a–d of Fig. 1 for the quantized component. The connected segments are now horizontal, and the y -values in panel b are integers.

According to Ref. [1], a background signal measured at 108 GPa was subtracted from the “Measured Voltage” in obtaining the published data (“Superconducting Signal”)

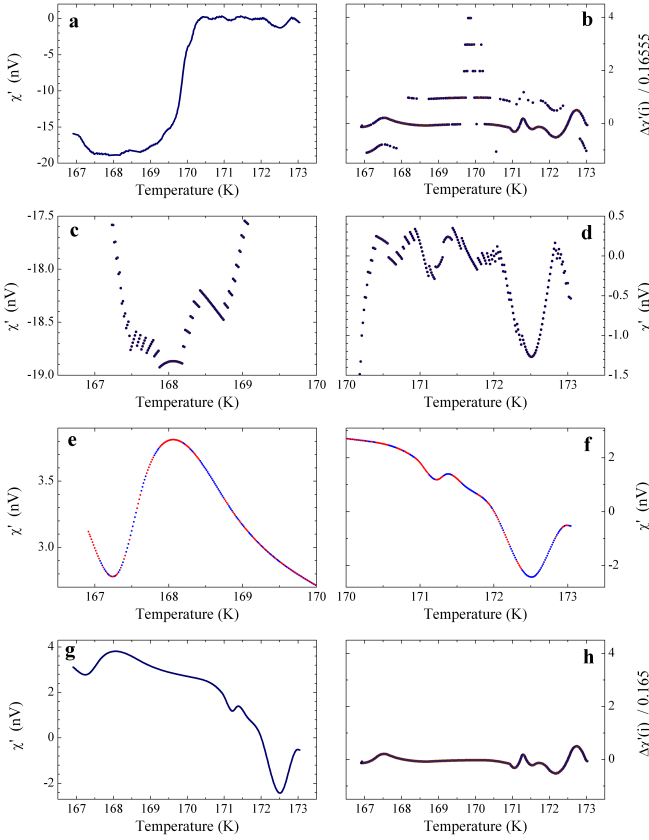


FIG. 1: **a**, Susceptibility data (“Superconducting Signal”) for CSH at pressure 160 GPa, from the numerical data of Table 5 of Ref. [2]. **b**, The difference between neighboring points of panel **a** divided by 0.16555. **c** and **d**, The data of panel **a** on an enlarged scale. **e**, **f** and **g**, The data of panels **c**, **d** and **a** after unwrapping with integer multiples of 0.16555. The different colors of panels **e** and **f** refer to disconnected segments of panels **c** and **d**. **h**, Same as panel **b** but now using the unwrapped data of panel **g**. The same vertical scale is used as for panel **b**.

in Ref. [1]. In other words,

$$\begin{aligned} \text{Superconducting Signal} &= \text{Measured Voltage} \\ &- \text{Background Signal} \quad (3) \end{aligned}$$

Comparison of Eq. (3) and Eq. (2) strongly suggests that the Measured Voltage and background signal in Eq. (3) correspond to the quantized component and $-1 \times$ unwrapped curve in Eq. (2) respectively.

III. A POSSIBLE EXPLANATION OF THESE RESULTS?

To begin to understand these results we have to understand (a) why the Measured Voltage deduced in section II (quantized component) is a series of flat steps separated by jumps of a fixed magnitude 0.16555 nV , and (b) why the background signal deduced in section II (the nega-

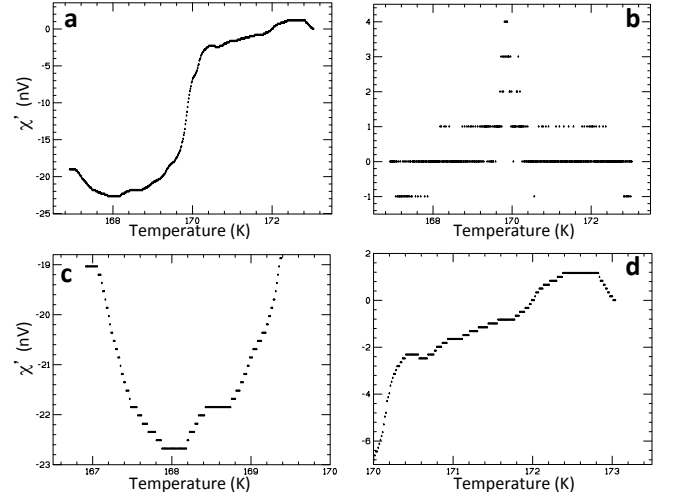


FIG. 2: **a**, Quantized component of susceptibility data (“Superconducting Signal”) for CSH at pressure 160 GPa. **b**, The difference between neighboring points of panel **a** divided by 0.16555. **c** and **d**, The data of panel **a** on an enlarged scale.

tive of the unwrapped curve) is a smooth curve with no experimental noise.

(a) A digital lock-in amplifier will yield discrete values for the measured voltages, where the size of the step between neighboring values of measured voltages is given by the instrumental resolution. Given our conclusion in section II that the quantized component shown in Fig. 2a could be the raw data (Measured Voltage), this would indicate that the resolution of the instrument in this measurement was of order 0.2 nV . Such a low resolution could result from setting the digitizer range of the lock-in amplifier to a large value, approximately $100 \mu\text{V}$ [7].

(b) The smooth behavior of the background signal ($-1 \times$ panel **g** of Fig. 1) could be explained if, rather than measured values of the background signal, a polynomial fit to the measured values was subtracted from the raw data. However, Ref. [1] does not mention such a procedure.

IV. BACKGROUND SIGNAL AND MEASURED VOLTAGE

In the previous section we have concluded that a possible way to understand the very unusual nature of the susceptibility data for 160 GPa reported in Ref. [1] could be if the measured raw data are the quantized component of the Superconducting Signal shown in panel **a** of Fig. 2, and the background signal is given by the negative of the unwrapped curve panel **g** of Fig. 1. On the other hand, the superconducting signal as well as the measured raw data were reported in Ref. [2] Table 5, and we can infer from them the background signal simply by subtraction.

Therefore, in Figs. 3 **a** and **b** we compare the reported raw data and the background signal inferred from the

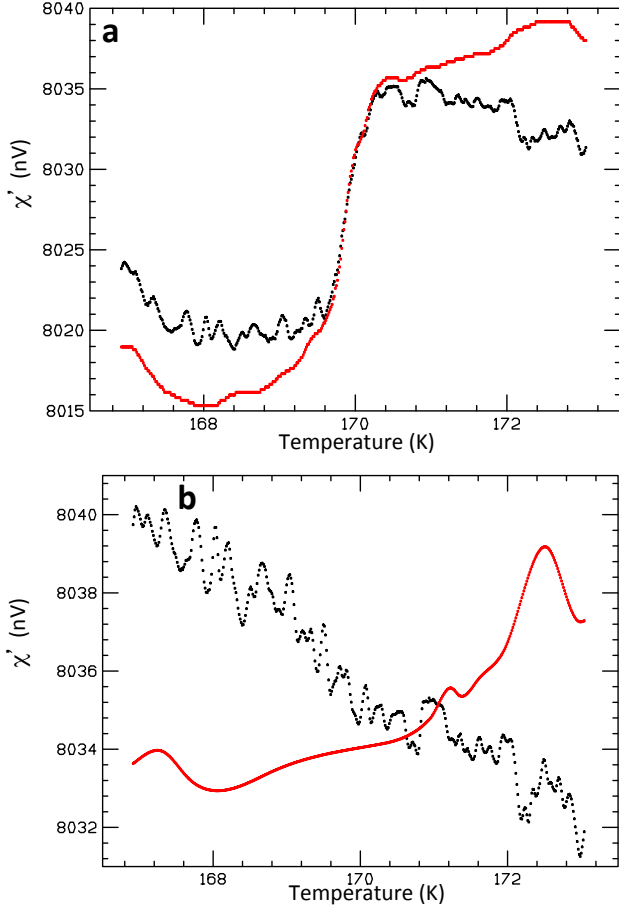


FIG. 3: **a**, “Measured Voltage” reported in Ref. [2] for 160 GPa (black points), compared with quantized component of susceptibility data (red points). **b**, Background signal inferred by subtraction of reported “Measured Voltage” and “Superconducting Signal” in Ref. [2] (black points), compared with background signal inferred from unwrapping of the susceptibility data (red points).

reported raw data and the reported data [2] with our hypothesized raw data and background signal deduced in section II.

It can be seen in Fig. 3 that there is a complete disconnect between the raw data and the background signal inferred from the numbers reported in Ref. [2], and the raw data and background signal inferred from the analysis of the Superconducting Signal [1] (numerical values given in Ref. [2]) discussed in section II. In particular, there is certainly no way that a polynomial fit of the black points in Fig. 3b would have any resemblance to the red curve shown in Fig. 3b, and there is a significant difference between the black and red curves in Fig. 3a.

There is also no quantization of measured voltages in the raw data reported in Ref. [2]. The reported measured values of the Measured Voltage are given in Table 5 of Ref. [2] with 11 significant digits. This is *not* necessarily the experimental resolution. The experimental resolu-

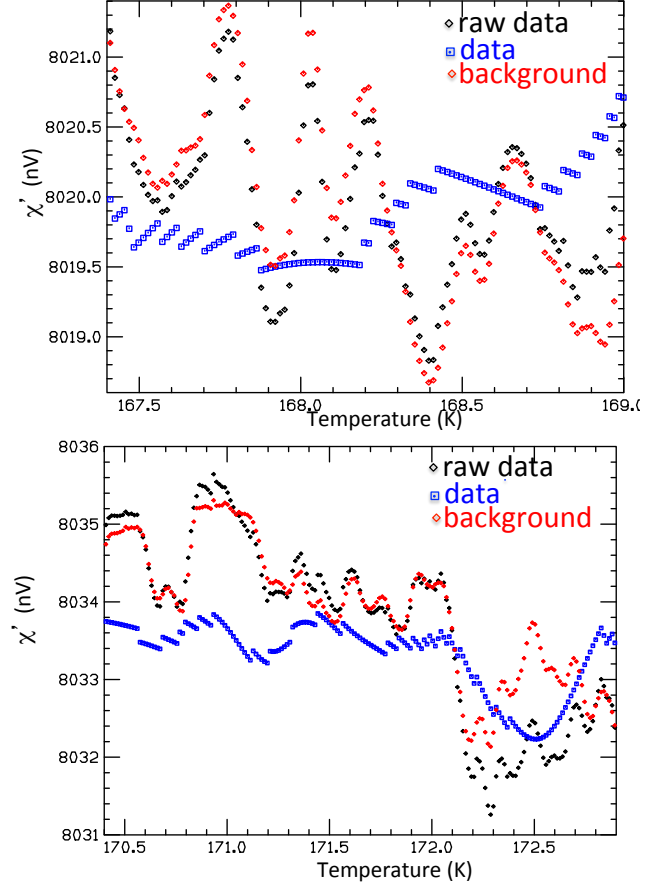


FIG. 4: Raw data, data and background signal inferred by subtraction, obtained from the numerical values reported in Table 5 of Ref. [2], for the low and high temperature regions of the 160 GPa data shown in panels c and d of Fig. 1.

tion is set by the complete analogue and digital chain of which the DAC is the last element. The smallest step between neighboring temperatures in Table 5 of Ref. [2] is of order 0.0001 nV. Hence the resolution of the experimental setup is 0.0001 nV or a smaller number. This is about three orders of magnitude higher resolution than the resolution of the measuring device that would yield the quantized component (red curve in Fig. 3a) as measured raw data.

It can also be seen in Fig. 3 that there is much larger noise in the raw data and background signal reported in Ref. [2] than there is in the red curves that were deduced from the reported Superconducting Signal in section II. The fact that the reported Superconducting Signal is significantly less noisy than the reported raw data was already noted in Ref. [5], not only for pressure 160 GPa but for all other pressures as well. This is independent of the unwrapping analysis discussed in the earlier sections. In Fig. 4 we show the raw data, the data, and the background signal obtained from the values reported in Table 5 of Ref. [2], for the low and high temperature parts of the 160 GPa data. It can be seen that in order

for the data (blue points) to result from subtraction of a background (red points) from raw data (black points) the oscillations in the background signal, presumably arising from instrumental noise, have to closely track oscillations in the raw data. Independently measured raw data and background signal do not have that property.

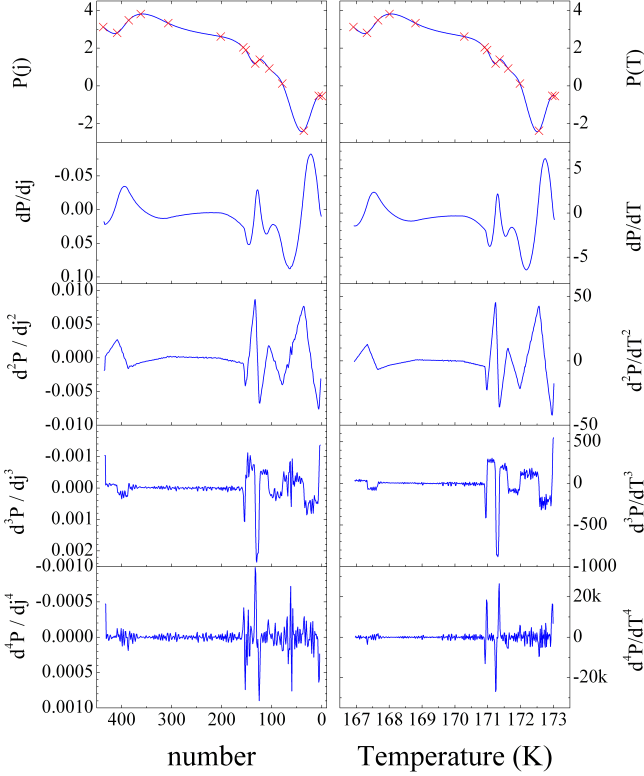


FIG. 5: From top to bottom: Unwrapped component of the susceptibility and it's first, second, third and fourth derivatives. Left panels: Numerical derivatives with respect to the row number. Right panels: Numerical derivatives with respect to the temperature. The parts of the curves between neighboring red crosses in the top panels are described by third order polynomials (see text for explanation).

V. PROPERTIES OF THE UNWRAPPED CURVE

The remarkable smoothness of the unwrapped curve obtained through the analysis in section II is illustrated by Fig. 5 where this curve is displayed together with the first, second, third and fourth derivate. The n 'th derivative of the j 'th point were calculated by applying the linear regression expression [12] to the $n - 1$ 'th derivatives at j and $j \pm 1$. Consequently the n 'th derivative can only be calculated for a smaller subset of points, namely $n \leq j \leq 437 - n$.

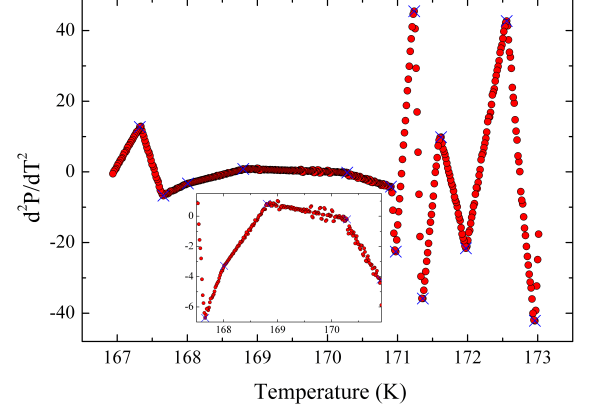


FIG. 6: Enlarged third right panel from the top of Fig. 5, showing the fourteen linear segments for the second derivative. The inset shows the center part enlarged further.

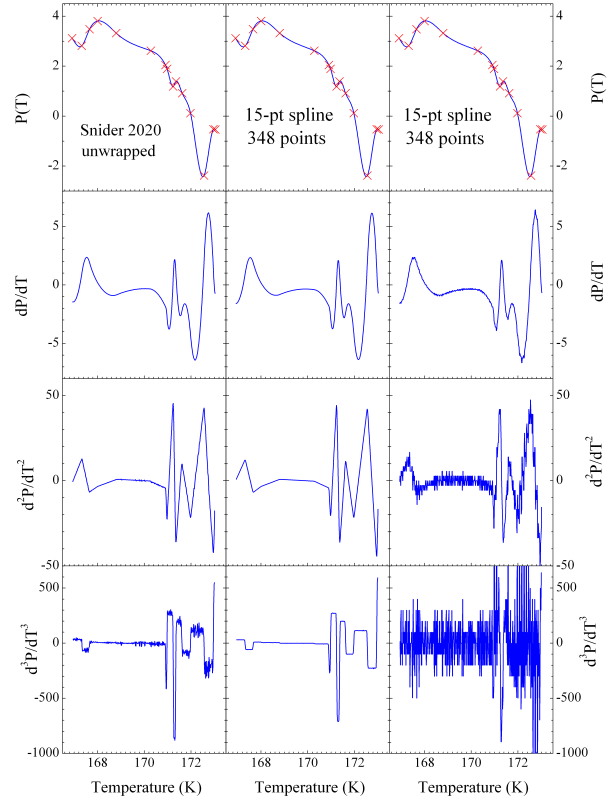


FIG. 7: Left from top to bottom : Unwrapped component of the susceptibility and it's first, second, and third derivatives. Right (middle) from top to bottom : 15-node cubic spline with natural boundary conditions generated with an older (newer) version of commercial plotting software and it's first, second, and third derivatives. The nodes are indicated as red crosses in the top panels.

segment	j_1	j_2	a	b	c	d
			nV	nVK ⁻¹	nVK ⁻²	nVK ⁻³
1	0	6	$-4.9708 \cdot 10^8$	$+8.61772 \cdot 10^6$	-49800.86194	+95.93123
2	6	36	$1.91612 \cdot 10^8$	$-3.32767 \cdot 10^6$	+19263.50719	-37.17133
3	36	79	$-7.45267 \cdot 10^7$	$+1.29874 \cdot 10^6$	-7544.15403	+14.60746
4	79	105	$7.3647 \cdot 10^7$	$-1.28653 \cdot 10^6$	+7491.41848	-14.54077
5	105	124	$-1.66029 \cdot 10^8$	$+2.90356 \cdot 10^6$	-16925.99285	+32.88943
6	124	133	$7.22616 \cdot 10^8$	$-1.26553 \cdot 10^7$	+73878.63337	-143.76142
7	133	152	$-2.28148 \cdot 10^8$	$+4.00122 \cdot 10^6$	-23390.90027	+45.58059
8	152	157	$3.8154 \cdot 10^8$	$-6.69719 \cdot 10^6$	+39185.38867	-76.42487
9	157	202	$4.9976 \cdot 10^6$	-88089.66243	+517.57022	-1.01366
10	202	307	565564.77819	-9977.32472	+58.67335	-0.11502
11	307	362	$-4.07314 \cdot 10^6$	+72452.65657	-429.58792	+0.84903
12	362	386	$-7.61789 \cdot 10^6$	+135753.45679	-806.38874	+1.59667
13	386	409	$4.96114 \cdot 10^7$	-888374.04134	+5302.58851	-10.55012
14	409	437	$-2.67393 \cdot 10^7$	+480488.75329	-2878.02049	+5.74622

TABLE I: Coefficients of the expression $\chi = a + bT_j + cT_j^2 + dT_j^3$ where T_j is the j 'th temperature for the 14 segments defined by $j_1 \leq j \leq j_2$. The coefficients were obtained by least square fitting the corresponding segments to a third order polynomial.

Only the fourth derivative is too noisy for readout. In the second derivative graph, shown in more detail in Fig. 6, all segments are straight lines. This clearly demonstrates that this curve is a chain of 14 polynomials of order 3. The curve, and its 1st, 2nd and 3rd derivatives fits the profile of a cubic spline [8] with 15 nodes. The nodes are shown as crosses in the top panels of Fig. 5 and in Fig. 6.

The temperatures are not equally spaced. To check whether the underlying functional dependence of the smooth curve is better described by temperature or by row number, the numerical derivatives with respect to T (right) are compared to those with respect to row number j (left) in Fig. 5. The noise level for third and fourth derivative in the right hand panel indicates that the 14 segments of the unwrapped curve are slightly less well described as functions of the row number than the temperature. The coefficients using the temperature representation are given in Table I. The noise level is the lowest for the offset in the range 0.16555 ± 0.00005 . Furthermore the 14 segments appear to be the output of a spline. The second derivatives extrapolate to zero at the extremal nodes, which corresponds to the so-called “normal” boundary conditions of the cubic spline [13]. This is the standard spline option of commercial plotting software. Applying the cubic spline with natural boundary conditions of different versions of commercial plotting software to the 15 nodes, and exporting on the temperature range defined by the two extremal nodes, gives the result in the middle and righthand panels of Fig. 7. The smaller noise of the middle column as compared to the right hand column (especially the third derivative) signals an improvement over time of the spline accuracy in subsequent versions of this software.

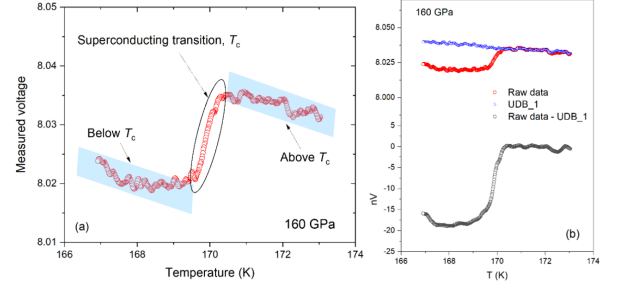


Fig. 2 AC susceptibility data. (a) Raw data measured at 160 GPa. The profile of the regions highlighted in blue are used as part of the UDB 1. (b) Measured voltage from the susceptibility measurement explained in experimental details section in Ref. 1 and 2 for 160 GPa. Raw data (red), UDB_1 (blue) and raw data - UDB_1 (black).

FIG. 8: Source: Fig. 2a of Ref. [10].

VI. FIRST PROTOCOL

According to Ref. [1]: “The background signal, determined from a non-superconducting C-S-H sample at 108 GPa, has been subtracted from the data”. Later in Ref. [10]: “We note here that we did not use the measured voltage values of 108 GPa as the background. We use the temperature dependence of the measured voltage above and below the T_c of each pressure measurement and scale to determine a user defined background.” The method illustrated in Fig. 2a of Ref. [10] is reproduced in Fig. 8. In particular it does *not* lead to the “superconducting signal” reported for 160 GPa, *i.e.* the superposition of a 15-node cubic spline and a quantized component. To introduce those two features in the “superconducting signal” requires that they are already present in the raw data, in the “user defined background”, or in both.

It will become possible to address the issues raised in Ref. [10] after the authors release the numerical values for their UDB1 (“user defined background method 1”) along with a detailed documentation of how this is derived -

and can be reproduced by others- from the experimental data.

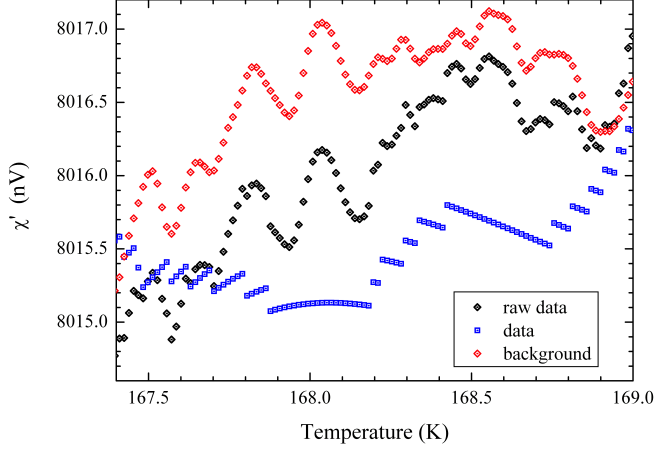


FIG. 9: Simulation of Eq. 4. Black: Measured Voltage. Red: Background Signal. Blue: Superconducting Signal.

VII. SECOND PROTOCOL

The inconsistencies pointed out in section VI do not occur when Eq. 3 is rearranged as follows:

$$\begin{aligned} \text{Measured Voltage} &= \text{Superconducting Signal} \\ &+ \text{Background Signal} \end{aligned} \quad (4)$$

This also removes the incongruences of the noise: The noise of “Measured Voltage” is now the sum of the noises of “Superconducting signal” and “Background signal” and therefore bigger than the noise of each of the latter two. A simulation is shown in Fig. 9, where for the Background panel an arbitrary curve was taken having a noise structure similar to that shown in Fig. 2a of Ref. [10] (also shown in Fig. 3b). Globally the features of “Measured Voltage” (red symbols) are similar to those in Fig. 4 upper panel. Despite differences in the noise structure, points in common of Fig. 4 and Fig. 9 are that (i) the “Measured Voltage” is noisier than “Superconducting Signal” and “Background Signal” and (ii) several (but not all) of the steps present in the “Superconducting Signal” also show up in “Measured Voltage”. In Fig. 10 we show the raw data points corresponding to connected segments of the data points identified by color and joined. It is apparent that several of the jumps in the data points are reflected in the raw data. This indicates that whatever the explanation is for the existence of these jumps in the data points has to also account for their existence in the raw data.

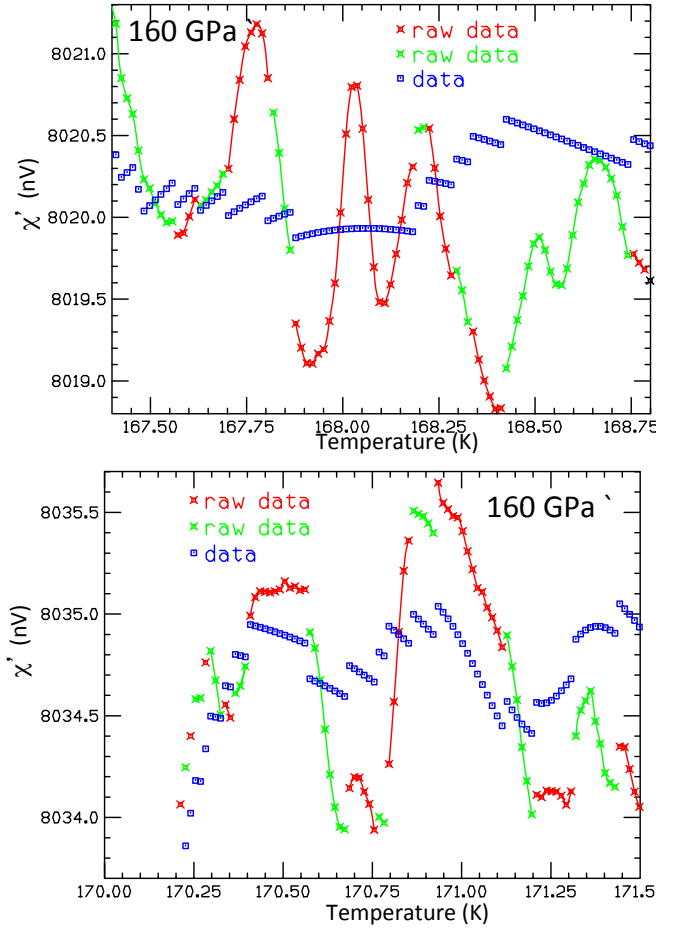


FIG. 10: Raw data and data obtained from the numerical values reported in Table 5 of Ref. [2], for low and high temperature regions of the 160 GPa data. Raw data points corresponding to each of the connected segments of the data points are identified by color (alternating red and green) and joined.

VIII. SUMMARY

The ac susceptibility reported in Ref. [1] was obtained by measuring the “Measured Voltage”, obtaining somehow [10] a “Background Signal”, and calculating from this the reported “Superconducting Signal” = “Measured Voltage” - “Background Signal”. In this manuscript we have analyzed in detail the published “Superconducting Signal” and “Measured Voltage” at 160 GPa.

- We have shown that the reported “Superconducting Signal” is the sum of two components: (i) A cubic spline with 15 nodes having “normal” boundary conditions at the two extremal nodes, and (ii) a quantized component with y values binned as $y = 0.16555n$ ($-7 < n < 138$).
- It is not clear what causes the quantization in increments of 0.16555 nV. The variation as a function of temperature of the “Measured Voltage” reported

in Ref. [2] occurs on a scale ~ 0.0001 nV which is three orders of magnitude below 0.16555 nV .

- The quantized component cannot be identified with the raw data since, other than containing the steep rise at 170 K, it departs strongly from the raw data reported in Ref. [2].
- The multi segment polynomial cannot be identified with the background signal, since it departs strongly from the difference “Measured Voltage”- “Superconducting Signal” according to the data reported in Ref. [2].

Readers interested to check the analysis resulting in Fig. 1 and Fig. 5 of this paper are welcome to download the corresponding excel tables from Ref. [6]. Numerical data for all pressures reported in Ref. [2] in image format are given in text format in Ref. [9].

Acknowledgments

We are grateful to Brad Ramshaw and Peter Armitage for stimulating discussions.

-
- [1] E. Snider, N. Dasenbrock-Gammon, R. McBride, M. Debessai, H. Vindana, K. Vencatasamy, K. V. Lawler, A. Salamat and R. P. Dias, “Room-temperature superconductivity in a carbonaceous sulfur hydride”, *Nature* **586**, 373 (2020).
- [2] R. P. Dias and A. Salamat, “Standard Superconductivity in Carbonaceous Sulfur Hydride”, *arXiv:2111.15017*, Dec. 28, 2021.
- [3] J. E. Hirsch, “Disconnect between published ac magnetic susceptibility of a room temperature superconductor and measured raw data”, doi: [10.20944/preprints202112.0115.v2](https://doi.org/10.20944/preprints202112.0115.v2).
- [4] J. E. Hirsch, “Incompatibility of published ac magnetic susceptibility of a room temperature superconductor with measured raw data”, doi: [10.20944/preprints202112.0188.v2](https://doi.org/10.20944/preprints202112.0188.v2).
- [5] J. E. Hirsch, “Superconductivity in Carbonaceous Sulfur Hydride: Further Analysis of Relation between Published AC Magnetic Susceptibility Data and Measured Raw Data”, doi: [10.20944/preprints202201.0003.v1](https://doi.org/10.20944/preprints202201.0003.v1); “On the room temperature superconductivity of carbonaceous sulfur hydride”, *Europhys. Lett.* doi.org/10.1209/0295-5075/ac50c9 (2022).
- [6] Excel files with the quantities shown in Fig. 1 and Fig. 5 are publicly available on <http://dirkvandermarel.ch/wp-content/uploads/chi.xlsx> and <http://dirkvandermarel.ch/wp-content/uploads/derivchnew.xlsx>.
- [7] Brad Ramshaw, private communication.
- [8] <https://en.wikipedia.org/wiki/B-spline>
- [9] Numerical values for all the data given in the tables of Ref. [2] are publicly available on <https://jorge.physics.ucsd.edu/cshdata.html>.
- [10] R. P. Dias and A. Salamat, “Reply to “Comment on Nature 586, 373 (2020) by E. Snider et al.””, *arXiv:2201.11883v1* (2022).
- [11] <https://timodenk.com/blog/cubic-spline-interpolation>
- [12] $y^{(n)}(j) = (S_x S_y - 3S_{xy}) / (S_x^2 - 3S_{xx})$ where $S_x = \sum_{i=j-1}^{j+1} x_i$, $S_y = \sum_{i=j-1}^{j+1} y_i^{(n-1)}$, $S_{xy} = \sum_{i=j-1}^{j+1} x_i y_i^{(n-1)}$, $S_{xx} = \sum_{i=j-1}^{j+1} x_i x_i$
- [13] A cubic spline smoothly connects n nodes with coordinates (x_j, y_j) ($1 \leq j \leq n$) by applying the condition of continuity of first and second derivatives at the $n - 2$ internal nodes. Two additional boundary condition are needed to fully define the spline function. Ref. [11] specifies the following types of additional boundary conditions: (i) Natural spline ($d^2y/dx^2 = 0$ at the two ends), (ii) Not-a-knot spline (d^3y/dx^3 are continuous for $j = 2$ and $j = N - 1$) (iii) Periodic spline (dy/dx and d^2y/dx^2 are equal for $j = 1$ and $j = N$) (iv) Quadratic spline (the first and the last segment are quadratic).